International Journal of Diabetes in Developing Countries (April–June 2025) 45(2):328–347
https://doi.org/10.1007/s13410-024-01377-7

ORIGINAL ARTICLE

An eccentric Iter Net–based Improved Intelligent Water Drop (I^2WD) feature selection and Discriminated Multi-Instance Classification (DMIC) models for diabetic retinopathy detection

Vinoth Rathinam[1] · Sasireka R[2] · K. Valarmathi[1]

Received: 7 December 2023 / Accepted: 11 July 2024 / Published online: 12 August 2024

Abstract

Background Diabetic retinopathy (DR) is an autoimmune disorder that affects the human eyes, causing lesions on the retina as a consequence of diabetes mellitus. Early identification of DR is crucial for effective vision maintenance and preventing severe vision loss.

Objective To develop and implement an automated and novel approach for the detection and classification of diabetic retinopathy, addressing the limitations of conventional DR detection systems which include complex disease detection, time-consuming processes, and low training efficiency.

Methods The proposed work introduces an Improved Intelligent Water Drop (I^2WD) optimization algorithm for selecting the most correlated features from the extracted feature set, thereby reducing the complexity of the classifier. For the prediction of DR, the Discriminated Multi-Instance Classification (DMIC) algorithm is employed, known for its higher accuracy and lower rate of incorrect predictions.

Results The proposed Item Net–based I^2WD-DMIC model is tested, validated, and compared using well-known benchmark datasets. The results demonstrate significant improvements in accuracy and efficiency over conventional DR detection methods.

Conclusion The novel I^2WD-DMIC approach offers a robust and efficient solution for diabetic retinopathy detection and classification, overcoming the typical limitations of traditional systems. This method shows promise in enhancing early diagnosis and improving patient outcomes in clinical settings.

Keywords Diabetic retinopathy (DR) detection · Retinal image · Preprocessing · Iter Net segmentation · Feature extraction · Improved Intelligent Water Drop (I^2WD) optimization · Discriminated Multi-Instance Classification (DMIC)

Introduction

Diabetic retinopathy (DR) damages the retinal blood vessels in patients with diabetes and is a major cause of blindness [1–3]. When a person has diabetes mellitus, their blood glucose levels often increase because the pancreas is unable to generate or release enough blood insulin. Typically, the DR is categorized into two types such as proliferated and non-proliferated, in which the non-proliferated DR is further categorized into the types of mild, moderate, and severe [4–6]. Moreover, diabetes is the most common cause of blindness in those who are 50 years of age or older. The condition known as diabetic retinopathy is a consequence of diabetes, characterized by destruction to retinal capillaries due to prolonged exposure to hyperglycemia. A little, round red dot at the terminal of blood arteries is called a micro-aneurysm (MA), which appears in the mild stage [7–9]. The MAs rip into lower retinal layers at the moderate stage, creating a hemorrhage that resembles a flame. More than 20 intraretinal hemorrhages in each of the four quadrants characterize the severe stage, which also includes obvious intraretinal micro-vascular anomalies and definite venous bleeding [10, 11]. But, the proliferation DR is a more advanced form of DR that result in revascularization, or the growth of functioning microvascular networks as new blood vessels on the retina's internal layer. In general, the normal and mild DR stages looks similar

✉ Vinoth Rathinam
vinoth@psr.edu.in

Sasireka R
sasivarun1304@gmail.com

K. Valarmathi
valarmathi@psr.edu.in

1 Department of Electronics and Communication Engineering, P.S.R. Engineering College, Sivakasi, Tamil Nadu, India

2 Department of Biotechnology, Mepco Schlenk Engineering College, Sivakasi, Tamil Nadu, India

[12, 13]; hence, it could be complex to identify the exact type. According to the recent survey, it is studied that nearly 595 million people can affect by DR at the year of 2025 [14–16]. The patients are unnoticed in the early stages of the DR, but it can proceed to cause floaters, vision impairment, imperfections, and gradual loss of vision. Therefore, finding the DR in its early stages might be challenging, but doing so is essential to preventing the serious consequences of later stages. The harmful vision loss brought on by DR mostly happens when there is central retinal edema. The International Report on Vision states [17] that nearly 12 million people around the world affected by vision impairment, due to the presence of DR. Consequently, creating an automated framework for DR detection and categorization is increasingly important and difficult. In conventional studies, various kinds of machine learning and deep learning algorithms [18–21] are applied for an automated DR detection with categorization. However, the shortcomings of the majority of learning models are their high system complexity, laborious task, and poor classification efficiency [22–24]. As a result, the proposed work aims to combine cutting-edge image processing techniques with a novel DR detection and classification framework. The following list includes the main goals of the suggested model:

- Initially, the input retinal image is preprocessed to create a quality-enhanced image, which includes the operations of uneven illumination removal, grayscale conversion, image de noising, and smoothening.
- The new deep learning–based Item Net architecture is then used to segment the retinal vessels with improved segmentation accuracy.
- Then, a clinical feature extraction algorithm is used for extracting well-suited features from segmented output, which includes the features of length, density, thickness, and tor touristy.
- After that, an Improved Intelligent Water Drop (I^2WD) optimization algorithm is used to choose the most correlated features from the available feature set.
- Finally, the Discriminated Multi-Instance Classification (DMIC) algorithm is deployed to predict the DR along with its stage.
- The performance and results of the proposed Iter Net–based I^2WD-DMIC technique is validated and compared by using the popular benchmarking datasets.

Continuing article is structured as follows: the "Related works" section presents the comprehensive assessment of the literature on the preprocessing, segmentation, feature extraction, and classification methods currently employed for DR prediction. It also examines the benefits and drawbacks of conventional algorithms based on how they operate during detection and classification. The explanation for the proposed Iter Net–based I^2WD-DMIC model is presented in the "Proposed methodology" section, along with the overview model, block diagram, and clear descriptions. The training and testing performance outcomes are reported in the "Results and discussion" section. In the "Conclusion" section, every aspect of the study is summarized together with the conclusions, results, and suggestions for the future.

Related works

The comprehensive literature review of the current models used for DR detection and classification is included in this part. It also considers the advantages and disadvantages of each model according to how effectively it operates and generates results for DR detection.

Qummar et al. [25] implemented an ensemble-based deep learning algorithm for DR detection. It combines the algorithms of bagging, boosting, and stacking, where the stacking is performed to incorporate the information from multiple prediction models. Typically, the stacking is one of the most suitable option for image classification, since it helps to improve the prediction rate of disease detection. Moreover, the authors normalized the imbalanced dataset for predicting the class label with high accuracy. However, this classification model requires more features for training and validation, which could degrade the results of the entire system. Alyoubi et al. [26] suggested a review to validate the different types of techniques used for DR detection. Atwany et al. [27] conducted a detailed investigation on various deep learning techniques used for DR detection. Here, the different types of DR are investigated, which includes MA, hemorrhages, and soft and hard exudates. In addition, it suggested some of the popular and recent public datasets for retinal image processing and DR detection. Moreover, the authors investigated both the binary class and multi-class prediction models for enhancing the performance of DR detection. Kandel and Castelli [28] suggested a transfer learning mechanism for DR classification. Different types of deep learning techniques are investigated to improve the process of DR detection. Also, the authors provided a complete architecture model for the CNN technique in order to design an effective classification model. Based on the study, it is analyzed that the sigmoid function, tan h, and ReLU activation functions are more essential in the deep learning model, since it helps to obtain increased classification accuracy. Kassani et al. [29] designed a modified X caption architecture model for categorizing the type of DR. The purpose of using this technique is to improve the discriminative ability of the feature extraction for obtaining improved classification accuracy. Moreover, the hyper-parameter tuning is performed to increase the performance of transfer learning mechanism. In this framework, the authors mainly concentrated on optimizing the training process of classifier by effectively preprocessing the input retinal image. During this process, the image resizing, minimum pooling, and normalization operations are carried out to produce the quality improved image. Shanthi and Sabeenian [30] utilized a modified AlexNet architecture for exactly categorizing the stages of DR.

Table 1 Survey on the existing techniques

Ref	Techniques	Dataset used	Pros and Cons
Huang et al. [31]	RT Net & Multi-lesion segmentation	IDRID and DDR	Improved efficiency for multi-tasking and increased segmentation accuracy
Sambyal et al. [32]	Modified U-Net segmentation	Indri and e-pother	Easy to optimize, ability to handle high-resolution images, and high system complexity
Hasan et al. [33]	DR Net segmentation	IDRID, RIMONE, and DRIVE	Better mean sensitivity, limited robustness, and over segmentation
Kumar et al. [34]	Optic disc segmentation	DIARETDB1	Training complexity due to increased number of features, better robustness and reliability
Xu et al. [35]	Feature Fusion U-Net (FFU-Net) segmentation	IDRID	Multi-scale feature fusion, and increased sensitivity

The authors aim to diagnose DR by implementing a deep learning mechanism. Table 1 presents the survey of various existing techniques used for DR segmentation and classification.

Materials and Methods

Study design

In this section, the proposed DR detection and categorization system is thoroughly explained. The main aim is to create an automated detection method that accurately predicts the kind of DR and its stage. This system uses cutting-edge and innovative image processing techniques to achieve the aforementioned objective. Figure 1a presents the suggested DR detection system's overview model, while Fig. 1b presents a clear flow illustration of the entire system. Here, the gathered retinal image is preprocessed at the beginning for producing the quality improved image. In order to produce a high-quality image, operations including grayscale conversion, image de noising, and smoothening are carried out at this step. After that, the retinal blood vessels were segmented using the cutting-edge deep learning–based segmentation model Iter Net to maximize the accuracy of DR detection and stage classification. Then, the segmented image is used to extract the most crucial clinical properties, including length, density, thickness, and tor touristy to increase detection efficacy. Once extracting the features, a novel and Improved Intelligent Water Drop (I^2WD) optimization algorithm is utilized to choose the well-suited and most correlated features through the available set of features. The purpose of implementing this feature selection algorithm is to reduce the complexity of DR detection system with low time consumption. Furthermore, the chosen features are fed to the classifier, named Discriminated Multi-Instance Classification (DMIC) model, for an accurate DR prediction and stage categorization. The major operations involved in the proposed model are listed in below:

- Image preprocessing
- Improved Iter Net segmentation
- Clinical feature extraction
- Feature optimization using I^2WD
- DR classification using DMIC

Image preprocessing

In this framework, the retinal color images are considered the input for processing, where the color enhancement is made to generate the normalized image. Generally, the retinal pictures comprise the RGB channels, and each of which having some distinct properties. In order to generate the grayscale image with high contrast, the RGB color channels must be properly managed. When compared to the color images, the grayscale images consume less time for processing. Moreover, the color images may comprise some irrelevant information, which may increase the amount of processing data required for segmentation or classification tasks. Hence, the grayscale conversion is performed in the proposed framework. After that, the uneven illuminations are removed from the grayscale image in order to enhance the recognition performance [36]. For this purpose, the morphological operations as well as homomorphism filtering processes are applied in the proposed framework. In which, the noise elimination and uneven illumination effects have been removed based on the morphological operations. The purpose of this approach is it raises the backdrop of the input with reduced noise artifacts. The mathematical representation of the bottom hat B_h operation is labeled in Eq. (1):

$$B_h(F) = F \bullet h - F \tag{1}$$

where the operator "•" indicates the closing operation. Consequently, the top hat operation $K_W(F)$ is performed to increase the contrast of the input image, which is represented in Eq. (2):

$$K_W(F) = F - F \circ h \tag{2}$$

By using these models, the problems such as uneven illumination as well as noise artifacts are effectively reduced. In addition, the homomorphism filtering mechanism is applied to generate the quality enhanced image, which includes the major components of

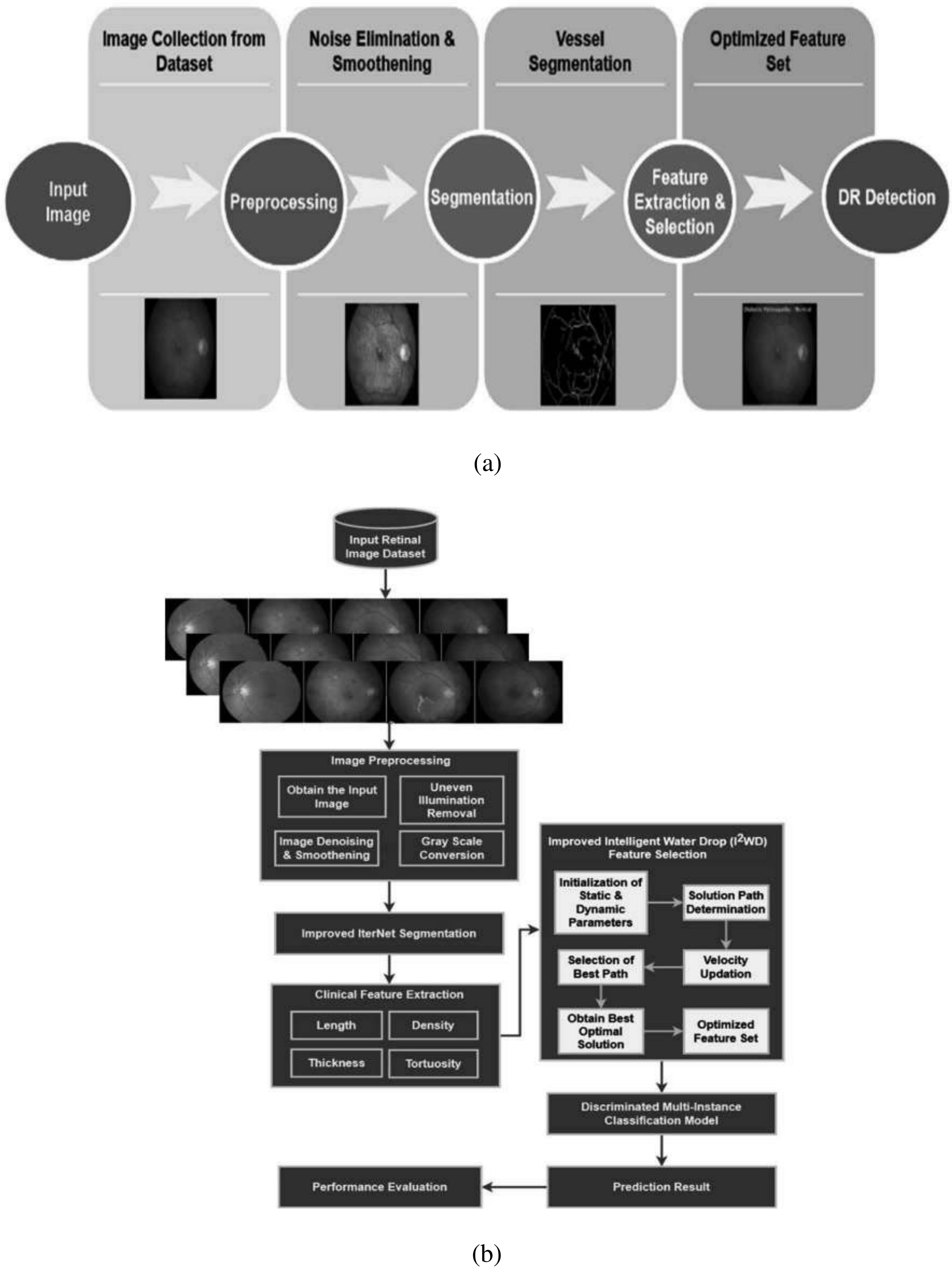

Fig. 1 **a** Overview of the proposed framework. **b** Flowchart of the proposed retinal image segmentation and classification system

illumination and reflectance. Moreover, the image is represented with these components as shown in the following models:

$$F(a,b) = \mathbb{M}(a,b) \times \mathbb{P}(a,b) \tag{3}$$

where $F(a,b)$ is the image representation, a, b are the pixel locations, and $\mathbb{M}(a,b)$ and $\mathbb{P}(a,b)$ are the illumination and reflectance components, respectively. Typically, the homomorphic filtering technique transforms the spatial image into a frequency image with the use of transformation functions. In addition, it uses the logarithmic functions $\mathcal{L}(F(a,b))$ for image transformation as presented in Eq. (4):

$$\mathcal{L}(F(a,b)) = \mathcal{L}(\mathbb{M}(a,b) \times \mathbb{P}(a,b)) \tag{4}$$

Moreover, the Fourier transformation derives the preprocessed image using Eq. (5):

$$FT(s(a,b)) = FT(\mathcal{L}(\mathbb{M}(a,b))) + FT(\mathcal{L}(\mathbb{P}(a,b))) \tag{5}$$

where $FT(.)$ indicates the Fourier transformation function. After image denoising, the quality improved image is produced as the output that is used for further segmentation and classification operations.

Improved Iter Net segmentation

Typically, segmentation of blood vessels is one of the most essential operations in the DR detection and classification system. For an accurate blood vessel segmentation, a novel Improved Iter Net segmentation algorithm is used in this work. Recently, the different kinds of deep learning–based image segmentation strategies [37] are applied in the traditional works for blood vessel segmentation, but they have the specific drawbacks of lower segmentation accuracy and low efficiency for the hard region images. Therefore, developing an accurate as well as effective blood vessel segmentation technique still remains one of the main challenging tasks. When compared to the other types of images, it is highly to obtain the large number of samples from the medical images like retinal images. Due to image acquisition, the retinal images may comprise a lot of noise, which hides the delicate vascular structure [38]. Moreover, the blood vessels are expanded rarely, and their orientation may change over time. These issues make segmentation more challenging in varying degrees, which often results in subpar outputs from the models. To avoid false predictions, the proposed technique uses an Improved Iter Net model for segmenting blood vessels from the preprocessed retinal image.

In this technique, a backbone network is constructed at first that comprises the U-Net input and output layers, and it adopts the encoding and decoding architecture. Moreover, this model could share the number of parameters for regularizing the model with reduced overfitting. Here, the edge preservation filter has been used to improve the features of the input image, which considers the preprocessed image PI as the input with the output guidance G, window ω_h, input X_h and output guidance, and G_h. It generates the output image as shown in the following form:

$$G_h = p_h PI_h + q_h \tag{6}$$

$$\delta_h := \sum_{i \in \omega_h} \left(\left(p_h PI_{h,i} + q_h - G_{h,i} \right)^2 + \tau p_h^2 \right) \tag{7}$$

where the parameters $p_h, q_h \in \mathfrak{B}$ are considered the coefficients of the window ω_h and τ indicates the normalization factor that helps to limit the magnitude of p_h. Then, the parameters p_h and q_h are computed by using the following models:

$$p_h = \frac{Cov\ (PI_h, G_h)}{Var\ \left(PI_h\right) + \tau} \tag{8}$$

$$q_h = \sum_{i \in \omega_h} \left(G_{h,i} - p_h PI_{h,i} \right) \tag{9}$$

At the time of training, the weight values of the input and output layers are updated, where the binary cross-entropy is estimated for pixel-wise segmentation that is represented as shown in the following equation:

$$BinE(G,M) = -1/rst\omega \sum_{i=1}^{r} \sum_{j=1}^{s} \sum_{h=1}^{t} \sum_{u=1}^{\omega} \left(G_{ijhu} \log M_{ijhu} + (1 - G_{ijhu}) \log (1 - G_{ijhu}) \right) \tag{10}$$

where the parameters r, s, t, ω are the batch size, number of image channels, height, and width of the image correspondingly. Then, the parameter M represents the ground truth image with the possible values of 0 and 1. Moreover, an Improved IterNet can produce the generated segmentation results according to the input and output layer of network architecture. Also, the actual loss function is estimated for each output class according to the ground truth label.

Clinical feature extraction

After segmentation, the clinical features are extracted from the segmented picture for improving the DR detection accuracy of the classifier. Typically, the clinical features are more useful for the medical practitioners for an appropriate diagnosis of DR. It includes the features of lesion thickness, length, density, and coefficient index value, in which the vessel length L_t is estimated according to the skeleton structure as shown in the following model:

$$L_t = \sum_{i=1}^{P-1} \sqrt{(k_{i-1} - k_i)^2 + (z_{i-1} - z_i)^2} \tag{11}$$

where P indicates entire pixels at the segmented skeleton and k_i and z_i are the pixel coordinates. Consequently, the vessel density D_t is estimated according to the image area as represented in the following equation:

$$D_t = \frac{\sum V_p}{S(mm^2)} \tag{12}$$

where V_p indicates the vessel pixels and S represents the size of image. Consequently, the tortuosity coefficient vector is estimated according to the degree of curvature and twists exist in the retinal blood vessels. It is computed by using the following model:

$$T_V\left(B_s\right) = \sum_{i=1}^{k} \frac{V_l(n)}{S_d(n)} \times n \tag{13}$$

where T_V indicates the tortuosity coefficient vector, B_s represents the blood vessel segment, V_l indicates the length of vessel, S_d is the straightforward distance among the ending points, and k denotes the branch of vessel segment. Then, the distance parameter S_d is estimated as represented in the following model:

$$S_d = \sqrt{\left(k_A - k_1\right)^2 + \left(z_A - z_1\right)^2} \tag{14}$$

where A represents the number of pixels in the blood vessels. In addition, the blood vessel thickness is also estimated according to its average value.

Improved Intelligent Water Drop (I^{2}WD) feature selection

After feature extraction, a novel I^{2}WD technique is implemented to prefer the most correlated features for maximizing the speed of training as well as classifier accuracy. Based on optimal solution obtained from I^{2}WD technique, the optimal count of features is selected and fed to the classifier for a proficient DR detection and type classification. Traditionally, many feature selection algorithms for DR detection and stage grading have been created in conventional works. The main advantages of utilizing the I^{2}WD methodology over other optimization methods include faster searching in the solution space, fewer iterations, low complexity, and high effectiveness. Typically, the proposed I^{2}WD technique is inspired by the natural river water flow model, where each drop operates independently as a separate agent that starts moving randomly with a certain velocity and a set initial soil value. Every drop that travels will pick up soil from the path's bed in proportion to its speed. Since water droplets always choose to follow the pool containing fewer soil, their shortest and most effective route will have less soil in it to attract other drops to follow it. In this technique, the graph having set of nodes and edges is constructed at first for resolving the given optimization problem, where a user-selected value set empirically based on an application is the quantity of soil present on each edge. Any two nodes with soil between them are first set as represented in the following model:

$$S_{i,j} = init^S \tag{15}$$

where i,j are the two nodes and S represents the initial amount of soil. After that, the static parameters such as total best solution $b(X^G)$; maximum number of iterations itr_{Mx}; current iteration C_{itr}; total number of water drop agents WD_{mx}; soil update parameters x_p, y_p, z_p; velocity updating parameters x_q, y_q, z_q; global parameter δ^{WD_N}; and soil updating parameter φ^n are initialized at the beginning of optimization. Similarly, the dynamic parameter like specific velocity $\wp^{WD}(l)$ is also initialized at first. In this model, each water drop can be transmitted via the present node i to the next consequent node j at the target space. To define the possible solution path of the network, the list of visited nodes is stored by water drop, as represented in the following model:

$$\{_i^{WD}(j) = \frac{F(soil)(i,j))}{\sum_{w\subseteq v(WD)}(F(soil(i,w)))} \tag{16}$$

where $\{_i^{WD}$ indicates the possible solution path. Moreover, the dynamic parameters are updated after transition of each drop. Then, the velocity updating function is represented as shown in the following model:

$$\wp^{WD}(l+1) = \wp^{WD}(l) + \frac{x_q}{y_q + z_q \ldots S^2(i,j)} \tag{17}$$

where $\wp^{WD}(\backslash\text{i} + 1)$ indicates the updated velocity function. Consequently, the amount of soil is computed according to the following function:

$$\Delta S(i,j) = \frac{x_p}{y_p + z_p \times t^2(i,j;\wp^{WD}(l+1))} \tag{18}$$

where t^2 indicates the time. Furthermore, the soil of path is updated among the nodes i and j as represented in the following model:

$$soil\ (i.j) = \left(1 - \{_n\right) \times S(i,j) - \{_n \times \Delta S(i,j) \tag{19}$$

At the end of iteration, the best path is selected that offers the optimal fitness value, and the best solution path X^G is identified by using the following model:

$$X^G = arg \underset{\forall X^{WD}}{max}\, b(X^{WD}) \tag{20}$$

where $b(.)$ indicates the best fitness function. Consequently, the selected paths on the soil are updated with the current best solution as shown below:

$$S(i,j) = (1 + \{_{WD}) \times S(i,j) \tag{21}$$

Finally, the optimal best solution path X^G is obtained as the output, which is used to choose the well-suited features from the retinal picture for improving the identification rate of DR.

Algorithm 1 Improved Intelligent Water Drop (I2WD) feature optimization

Input: Extracted feature set;

Output: Optimal best solution path X^G;

Step 1: Initialize the static input parameters such as total best solution $b(X^G)$, maximum number of iterations itr_{Mx}, current iteration C_{itr}, total number of water drop agents WD_{mx}, soil update parameters x_p, y_p, z_p, velocity updating parameters x_q, y_q, z_q, global parameter δ^{WD_N}, and soil updating parameter φ^n;

Step 2: Initialize the dynamic input parameter $\wp^{WD}(l)$;

Step 3: During transmission from one node to another node, each drop can maintain the list of visited nodes for computing the possible solution as shown in equ (16);

Step 4: Consequently, the dynamic parameter $\wp^{WD}(l+1)$ is updated by using equ (17);

Step 5: Then, the amount of soil is estimated $\Delta S(i,j)$ with the static parameters and velocity as shown in equ (18);

Step 6: Moreover, the soil of path is updated between the nodes i and j by using eqn (19);

Step 7: The best optimal solution path is determined X^G using equ (20);

Step 8: Based on the selected paths, the current best solution path is estimated using eqn (21);

Step 9: For each iteration,

$$X^G = \begin{cases} X^G & \text{is } b(X^G) \geq b(X^G) \\ X^G & \text{Otherwise} \end{cases} \tag{22}$$

End for;

Step 10: Return the best optimal solution as X^G;

Discriminated Multi-Instance Classification (DMIC)

After feature selection, the DMIC algorithm is employed to predict the DR from the given retinal imageries with high accuracy. The earlier studies typically used a variety of machine learning with deep learning algorithms for efficient DR recognition, segmentation, and categorization. However, the majority of approaches are constrained by the unique issues of increased training complexity, lengthy computation times, poor system performance, and high false-positive rates [39, 40]. In order to identify DR and classify stages, the suggested work aims to construct a novel multi-instance learning-based classification system. The main scope of using this technique is to reduce the segmentation and classification burden of ophthalmologist by performing mapping between the instances and labels. Here, the classifier is trained on the target domain for predicting the bag of labels from the retinal images. The novel contribution of this methodology is that it uses the multi-instance learning model incorporated with an attention mechanism for better and accurate image DR recognition and classification. During this process, the relationship is identified for determining the mapping between the instances and labels. Here, an attention mechanism is incorporated to improve the learning operation. The weight value of the instance is updated using an attention mechanism as represented in the following model:

$$\tau_j^{(j)} = \frac{exp\left\{\omega^t(\tanh(\beta(\mathrm{A}_i^j)^t\right\} \odot sign(G(\mathrm{A}_i^j)^t))\}}{\sum_{h=1}^{\rho}\exp\{\omega^t(\tanh(\beta(\mathrm{A}_i^j)^t\} \odot sign(G(\mathrm{A}_i^j)^t))\}} \tag{23}$$

where A_i^j indicates an instance embedding; $\tau_j^{(j)}$ represents the attention weight; ω^t, β, and G are the learned parameters; h is the class number; and ρ indicates the patch size of bag. By using the optimized weight function, the corresponding class is predicted as represented in the following model:

$$\widehat{A}_i^{(j)} = \tau_j^{(j)} A_i^{(j)} \tag{24}$$

where $\widehat{A}_i^{(j)}$ indicates the instance embedding dimensionality. Then, the instance embedding is concatenated with the attention weight value as represented in the following model:

$$\widehat{CA}_i = concat[\widehat{A}_i^{(1)}, \widehat{A}_i^{(2)} \ldots \widehat{A}_i^{(\rho)}] \tag{25}$$

In addition, the multi-class entropy M_E loss function is estimated by using the following equation:

$$M_E = -\frac{1}{I_T}\sum_{i=0}^{I_T}\sum_{g=0}^{G}(s_{i,g}^t \times \log(\widehat{s_{i,g}^t})) \tag{26}$$

where I_T indicates the total number of images, G represents the grade of DR, $s_{i,g}^t$ implies the severe grade of DR, and $\widehat{s_{i,g}^t}$ denotes the estimated class label. By using this algorithm, the DR is detected along with its grade. Figure 2 shows the sample input and output retinal images.

Results

With the use of benchmarking datasets including DIARETDB1, MESSIDOR, IDRID, Kaggle, and EyePACS, the proposed Iter Net–based I^{2}WD-DMIC mechanism's results are presented in this section along with a description of the process. Additionally, the test results of the suggested DR detection framework are evaluated using a variety of evaluation indicators. The aforementioned datasets are extensively used in many DR detection applications for validating the training and testing efficiency of the prediction models. Additionally, the following models are utilized to calculate the various types of measurements needed for validating the training and testing performance of the classification system:

$$Accuracy = \frac{Tp + Tn}{Tp + Fp + Tn + Fn} \tag{27}$$

$$Sensitivity\ or\ recall = \frac{Tp}{Tp + Fn} \tag{28}$$

$$Specificity = \frac{Tn}{Tn + Fp} \tag{29}$$

$$Precision = \frac{Tp}{Tp + Fp} \tag{30}$$

$$F1 - score = \frac{2 \times Precision \times Recall}{Precision + Recall} \tag{31}$$

Consider Tp as true positives, Tn as true negative, Fp as false positive, and Fn as false negative.

The resulting confusion matrix for the IDRID database is shown in Fig. 3. The confusion matrix typically displays the performance and accuracy of the classifier, with the greater true positive outcomes showing the classifier's high performance. Additionally, Fig. 4 displays the results of the proposed Iter Net–based I^{2}WD-DMIC model's performance study using the MESSIDOR dataset.

By using the EyePACS dataset, Fig. 5 compares the effectiveness of the proposed Iter Net–based I^{2}WD-DMIC mechanisms to the performance of the standard deep learning methods [41]. Consequently, the performance of some other deep architecture models is compared with the proposed Iter Net–based I^{2}WD-DMIC technique by using MESSIDOR dataset as shown in Fig. 6. Due to imaging activities such as preprocessing, Iter Net segmentation, clinical feature extraction, I^{2}WD feature optimization, and DMIC classification,

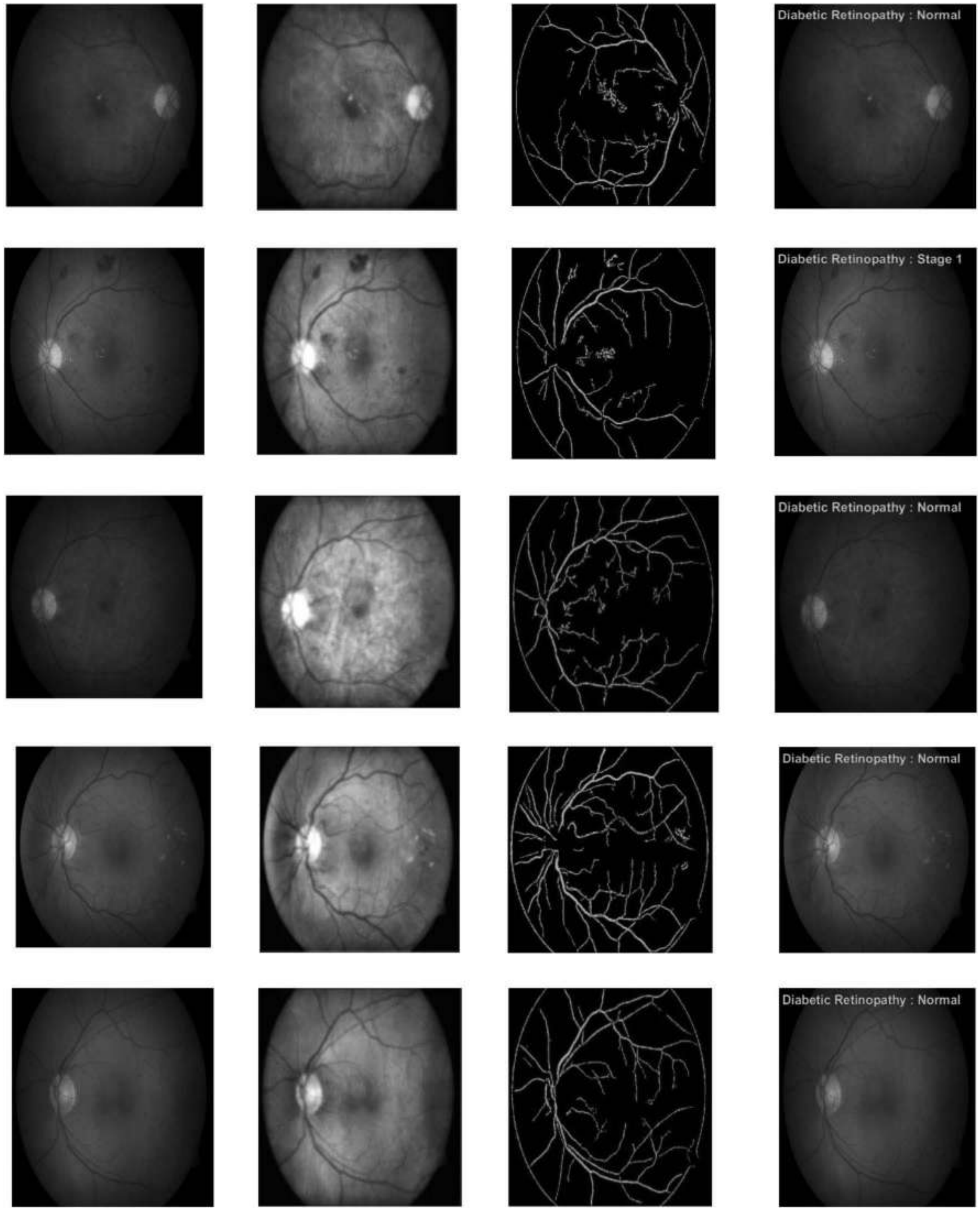

Fig. 2 Sample images: **a** Input image, **b** preprocessed image, **c** segmented region, and **d** predicted result

the proposed DR detection mechanism improves performance outcomes for all the datasets employed in this study.

The proposed DMIC model's ROC is validated in Fig. 7a, b with regard to various classes of DR. Based on the analysis, it is found that the ROC is significantly better for all classes of DR. The true positive rate has significantly increased in the proposed system as a result of the addition of Iter Net segmentation and I^2WD optimization approaches.

Figures 8, 9, and 10 validate the accuracy, sensitivity, and specificity [42]. Here, the performance is assessed in accordance with the various numbers of imageries. The findings show that, in comparison to previous classification

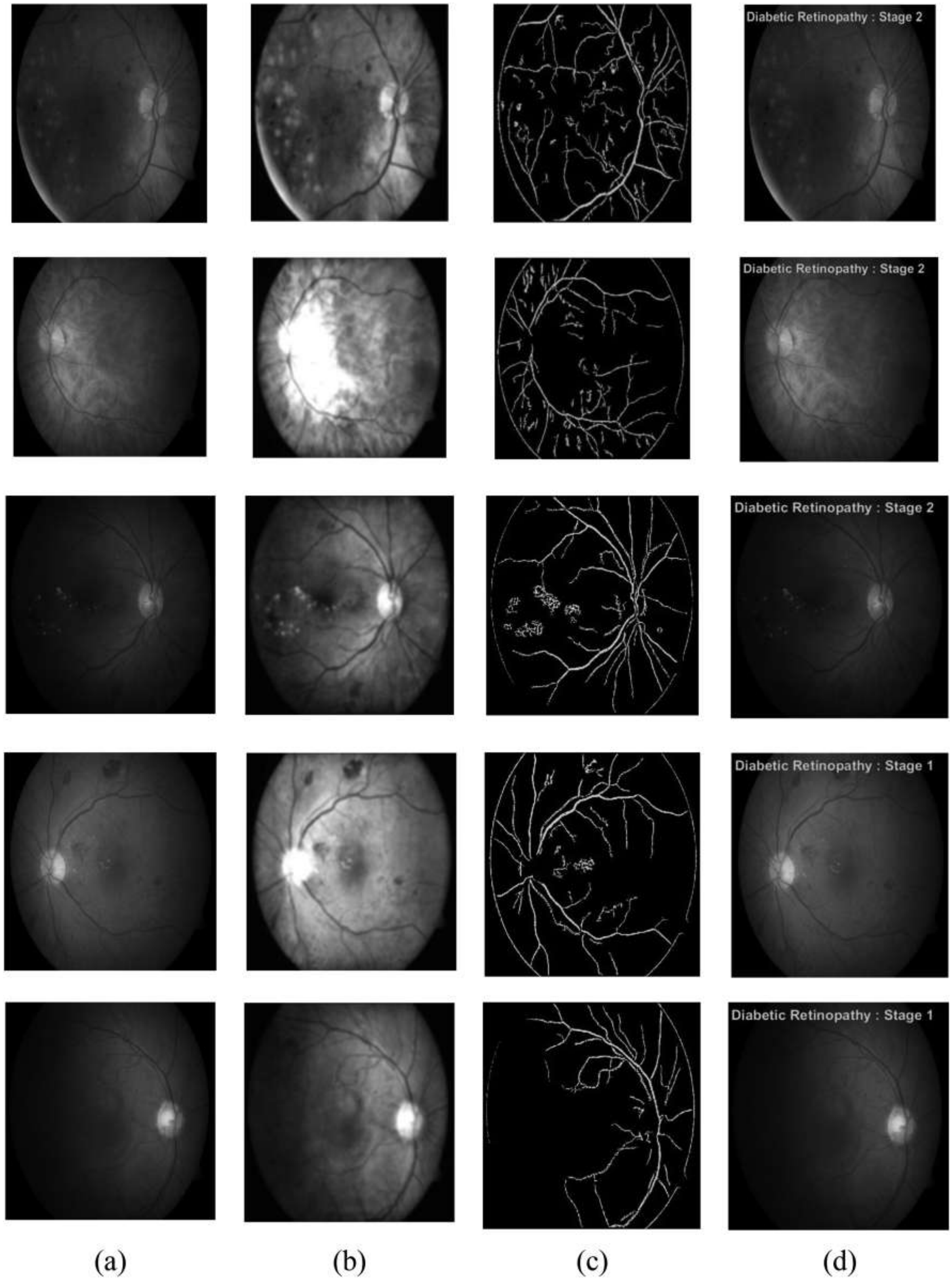

Fig. 2 (continued)

techniques, the proposed Iter Net–based I^{2}WD-DMIC technique offers higher accuracy, sensitivity, and specificity values.

Figure 11 validates and compares the entire presentation of the existing feature extraction-based classification and proposed Iter Net–based I^{2}WD-DMIC models by using the

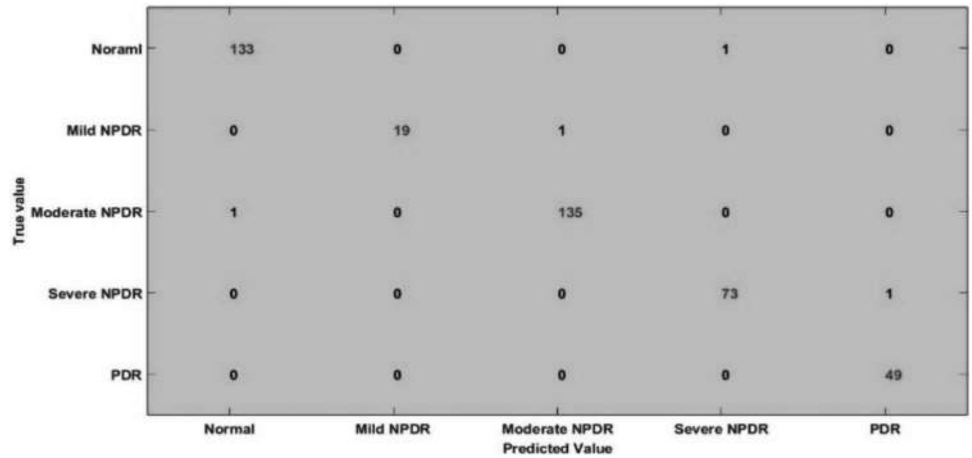

Fig. 3 Confusion matrix for IDRID dataset

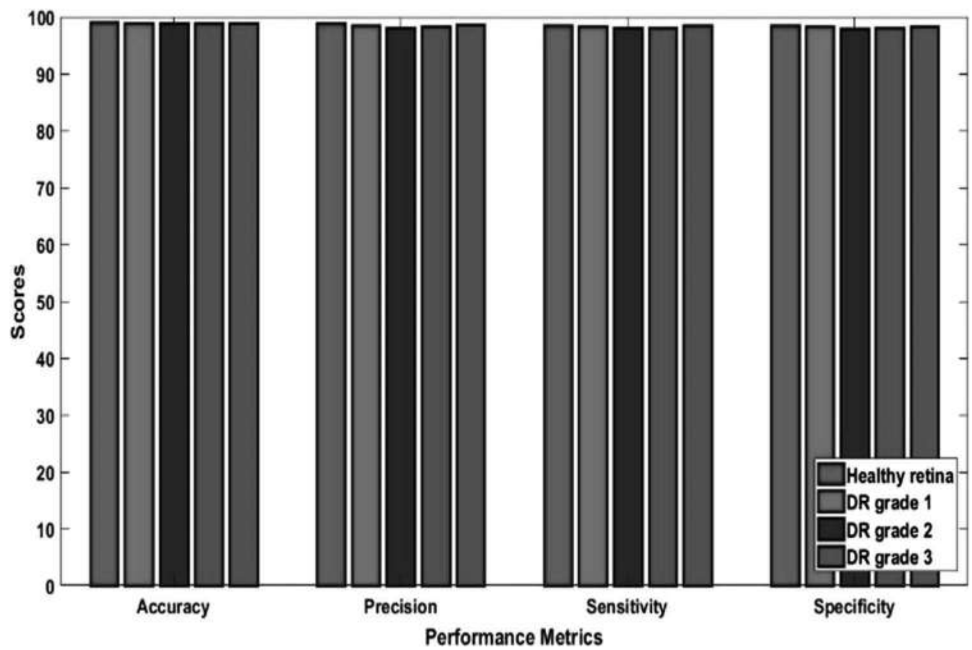

Fig. 4 Performance analysis of the proposed Iter Net–based I^2WD-DMIC

DIARETDB1 dataset. Typically, feature extraction is crucial to the automated DR detection system since it enhances the classifier's training and testing processes. Therefore, it is more important than ever to take the most relevant and suitable features from the provided retinal images. To extract the appropriate characteristics from the segmented retinal picture, the suggested study employs the clinical feature extraction model. The I^2WD optimization algorithm is then used to further optimize the collected features, significantly reducing the complexity of classification while enhancing training efficiency. As a result, the suggested Iter Net–based I^2WD-DMIC offers better performance outcomes than other methods.

Figure 12 validates the accuracy of the proposed Iter Net–based I^2WD-DMIC mechanism with respect to varying number of epochs. The results indicate that the accuracy of the proposed DR detection framework is greatly increased with the use of Iter Net image segmentation mechanism.

Figure 13 validates the accuracy and *K*-score values of the conventional machine learning [43] and proposed Iter Net–based I^2WD-DMIC mechanism by using IDRID dataset. The results show that, in comparison to existing machine learning models, the suggested DR detection model offers higher accuracy and *K*-score values.

Figures 14, 15, and 16 present the performance of the existing machine learning such as SVM, RF, MLP, and proposed Iter Net–based I^2WD-DMIC models by using three different datasets such as IDRID, MESSIDOR, and Kaggle, respectively.

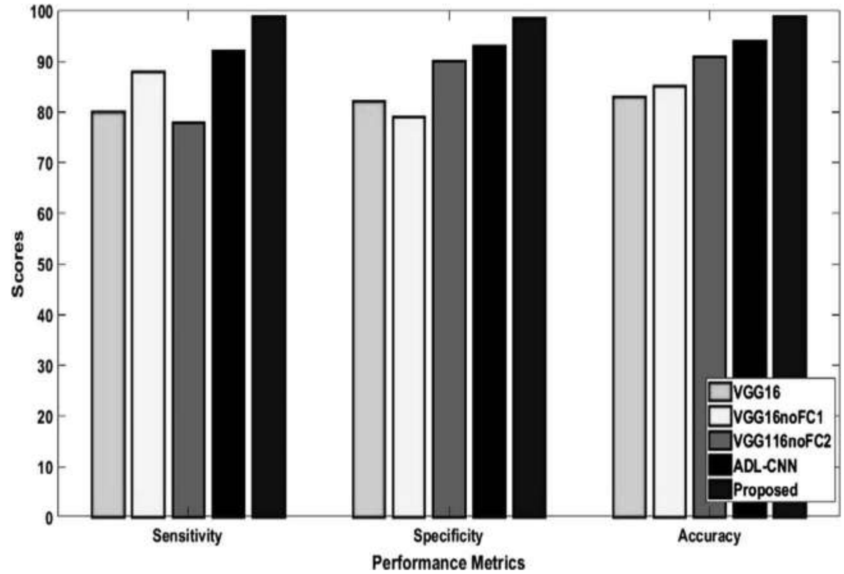

Fig. 5 Performance comparative analysis using EyePACS dataset

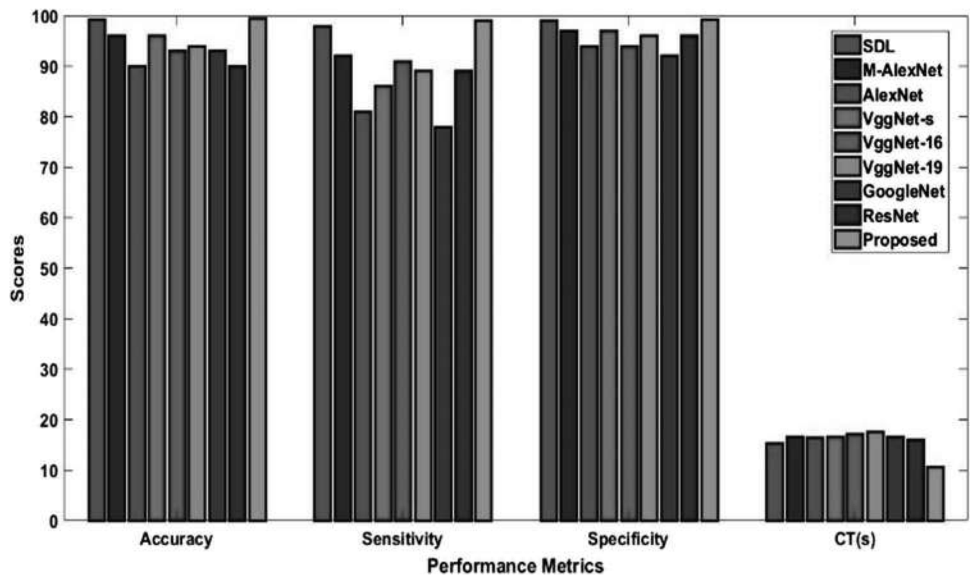

Fig. 6 Comparative analysis using MESSIDOR dataset

Figures 17, 18, and 19 show the false-positive rate of the existing and proposed DR detection models for the IDRID, MESSIDOR, and Kaggle datasets, respectively.

Discussion

The various performance indicators are taken into consideration in this research to show how the suggested framework has enhanced DR detection performance and efficiency. Overall, the results show that, in comparison to previous machine learning models, the suggested DR detection approach offers better performance outcomes. The suggested DMIC model successfully integrates IterNet segmentation and I2WD optimization to accurately anticipate the DR and its stage. Here, the clinical feature extraction and I2WD feature selection models are the specific reasons for obtaining the reduced false positives, since the classifier's training operation is effectively improved with the use of optimized feature set. The reduced false positive rates are achieved by the proposed IterNet-based I2WD-DMIC mechanism for all the three datasets namely IDRID, MESSIDOR, and Kaggle.

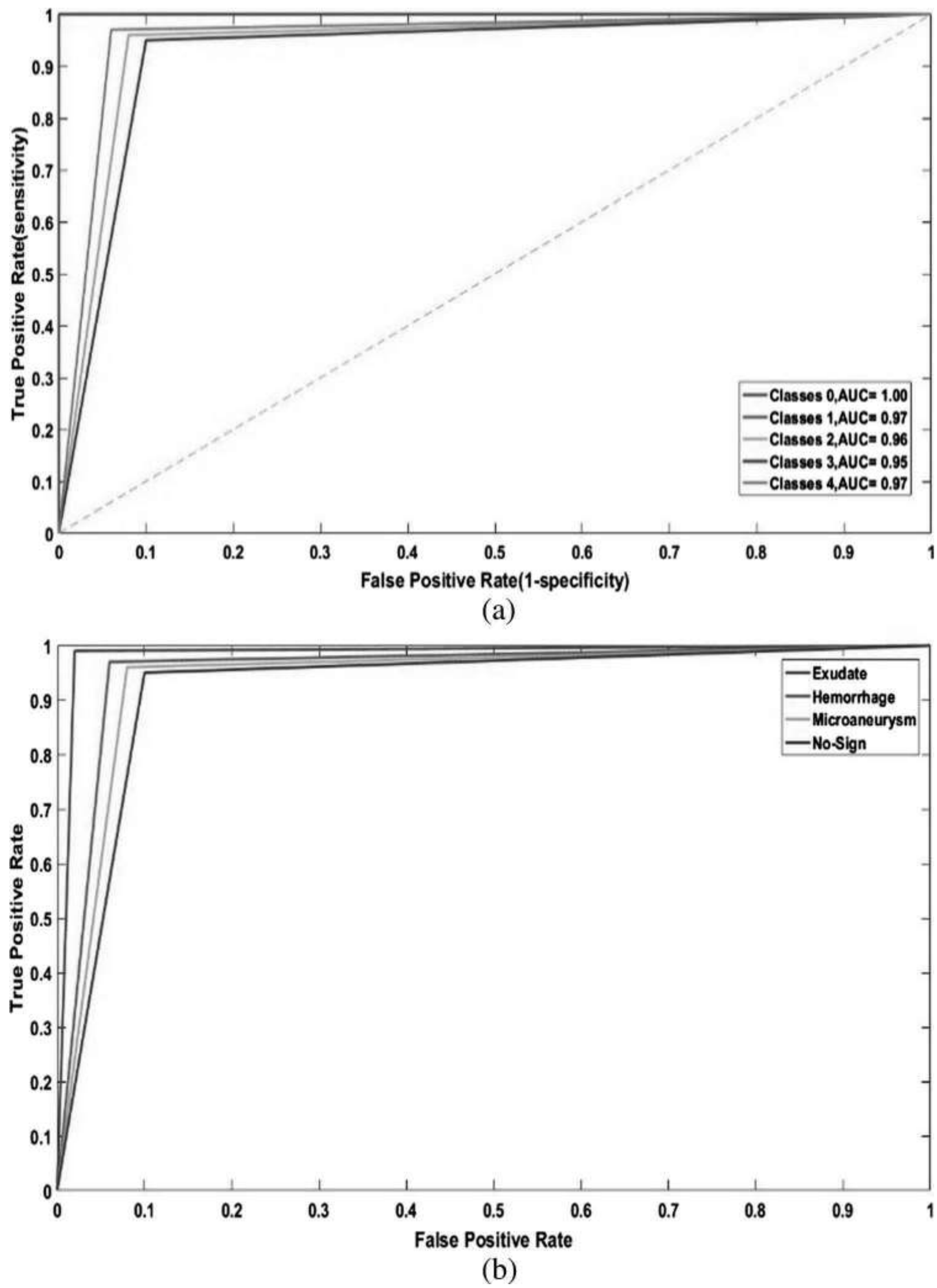

Fig. 7 **a** ROC–AUC analysis with different types of DR classes. **b** ROC analysis with different classes of DR

Conclusion

This research introduces a unique Iter Net–based I^2WD-DMIC framework for DR identification with categorization. The primary aim is to the creation of a highly effective, automated technique for DR detection. This framework implements a variety of image processing methods for this purpose. Here, the collected retinal image is first preprocessed to create the higher-quality image. At this stage, processes like grayscale conversion, picture de noising, and smoothening are completed to create a high-quality image. The retinal blood vessels are divided into distinct groups using state-of-the-art deep learning–based segmentation model Iter Net to increase the precision of DR detection and stage categorization. The most important clinical attributes, such as length, density, and thickness, are extracted from the segmented image to enhance the detection performance. The well-suited and most associated features are selected from the available set of data using novel I^2WD optimization technique once the features have been retrieved. The major goal of putting this feature selection

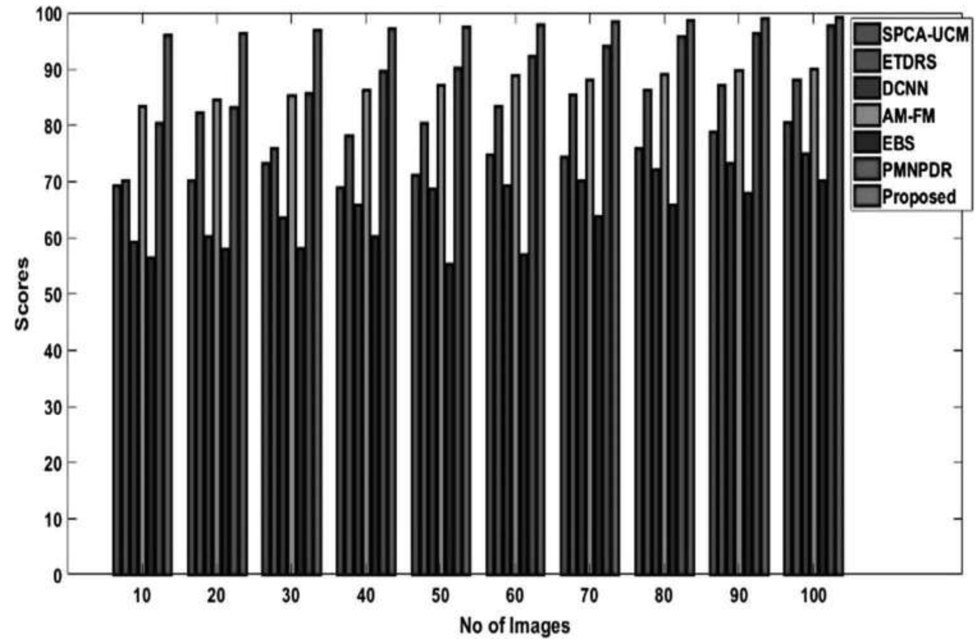

Fig. 8 Accuracy analysis with respect to different number of images

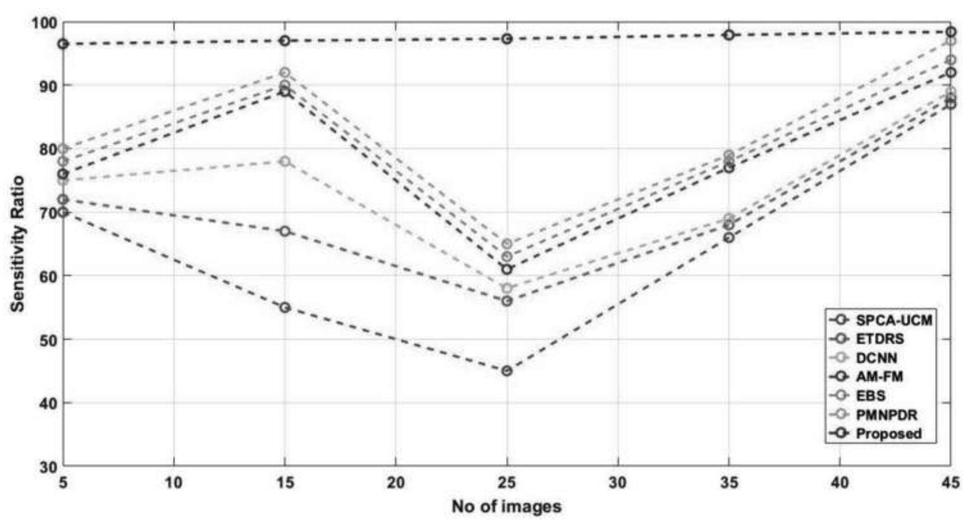

Fig. 9 Sensitivity ratio vs no. of images

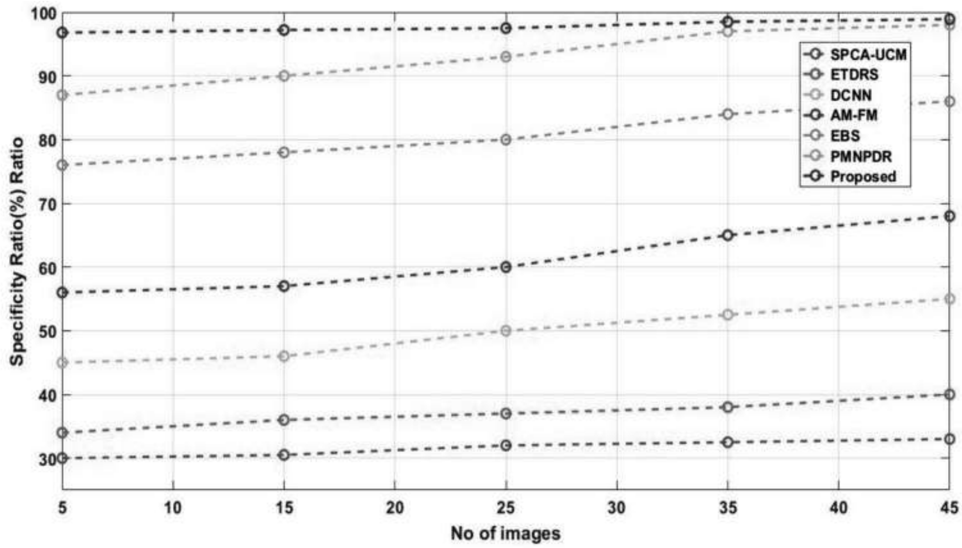

Fig. 10 Specificity ratio vs no. of images

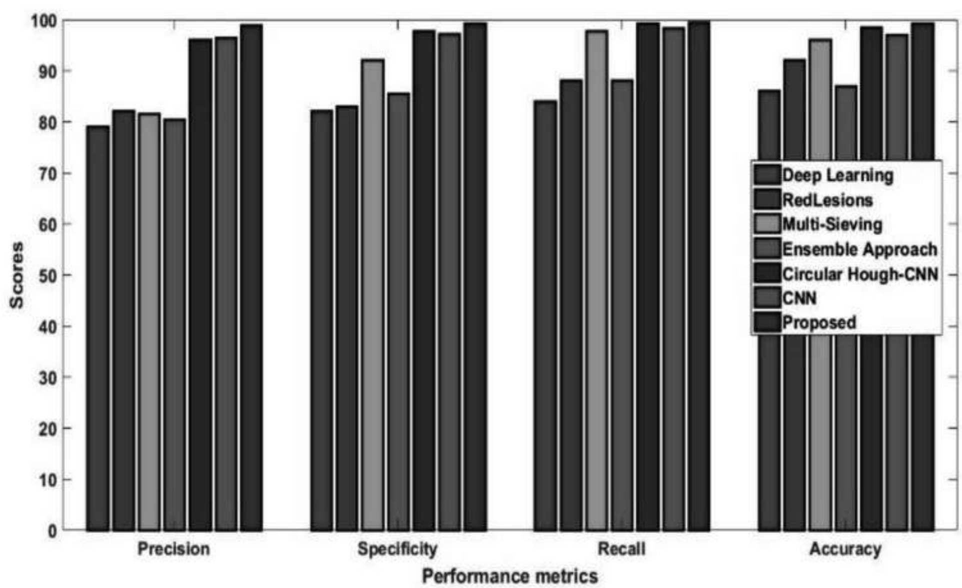

Fig. 11 Overall performance analysis

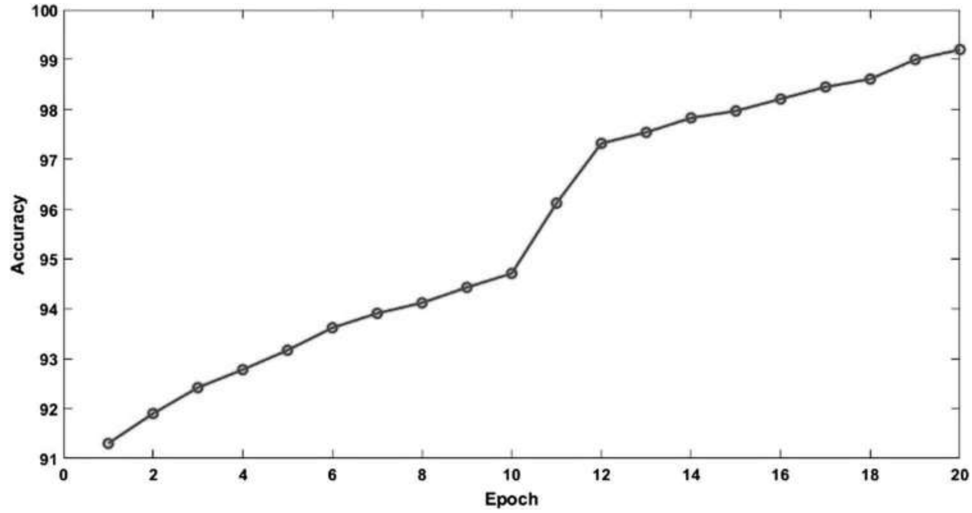

Fig. 12 Accuracy of the proposed model with varying epochs

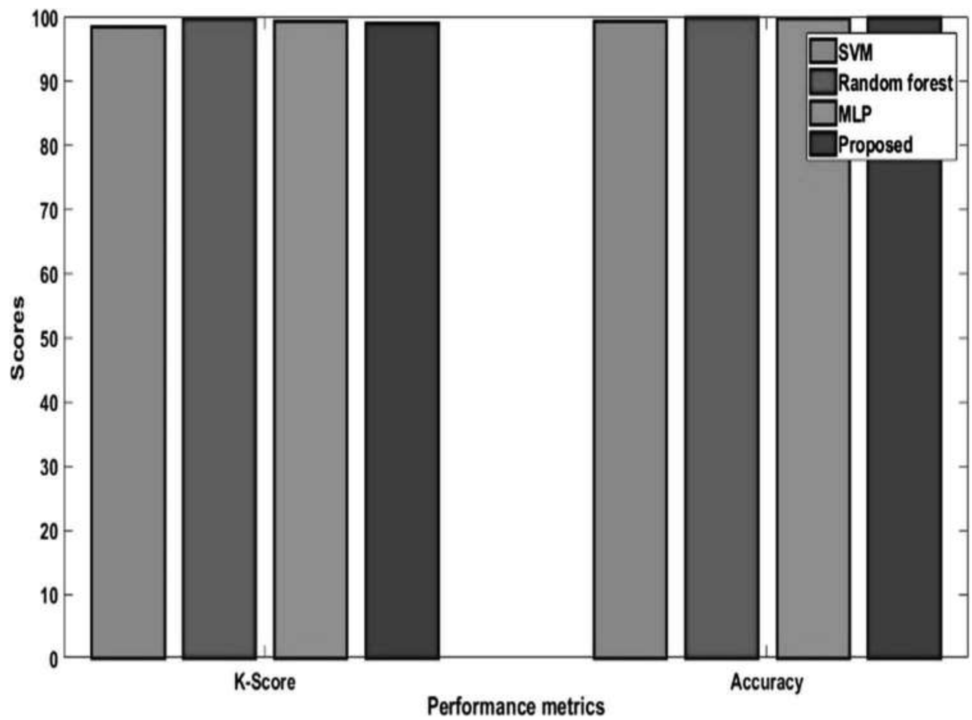

Fig. 13 *K*-score and accuracy analysis with other machine learning models using IDRID dataset

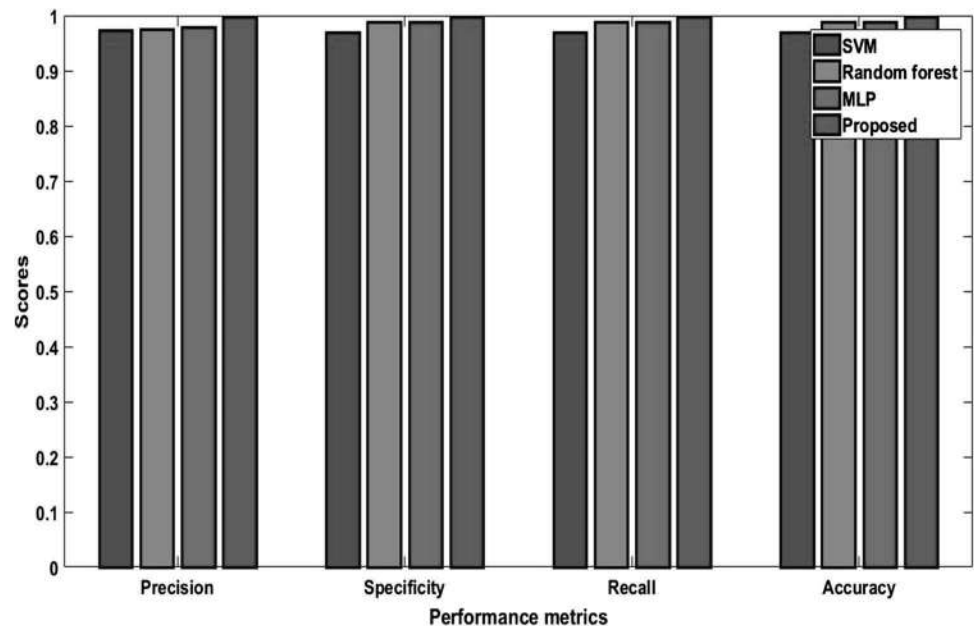

Fig. 14 Performance of proposed and other machine learning methods using IDRID dataset

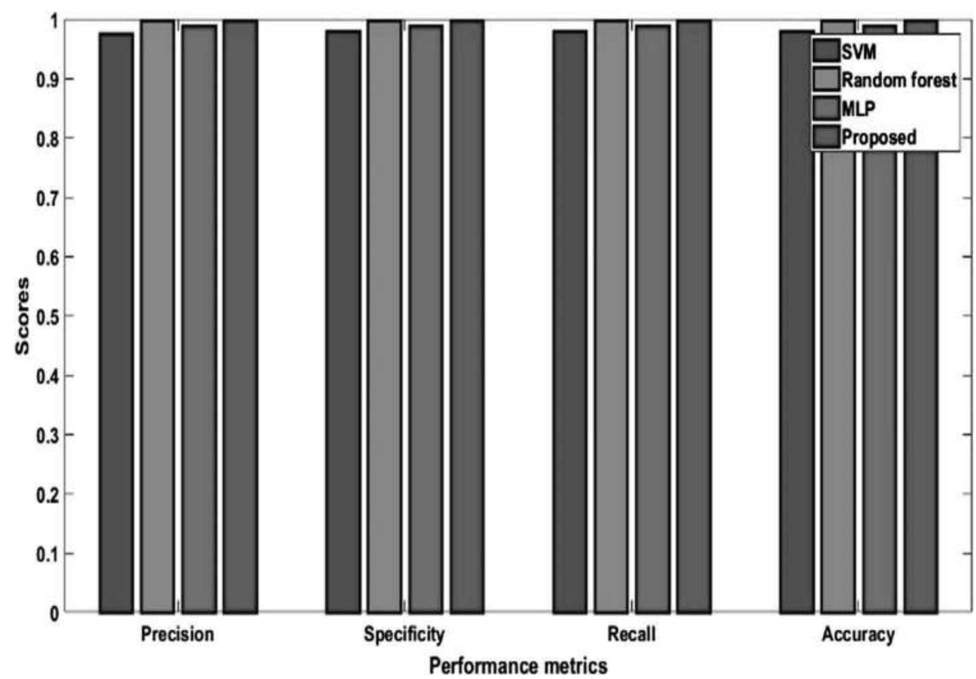

Fig. 15 Performance of proposed and other machine learning methods using MESSIDOR dataset

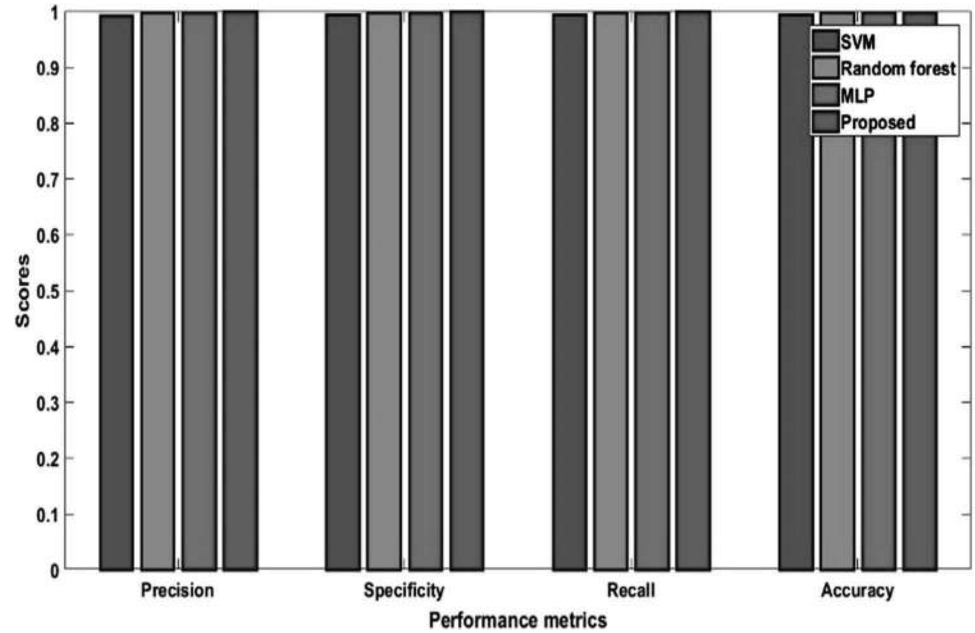

Fig. 16 Performance of proposed and other machine learning methods using Kaggle dataset

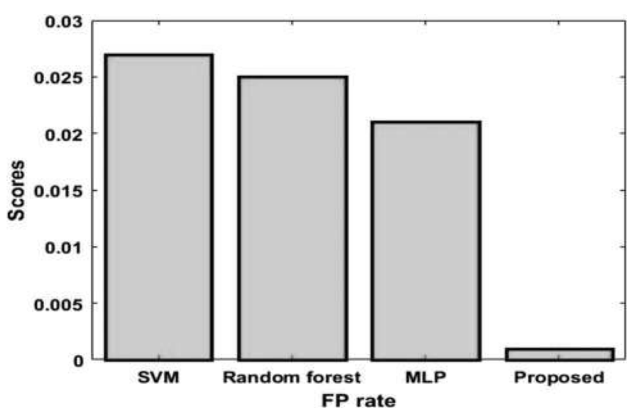

Fig. 17 False-positive rate analysis using IDRID dataset

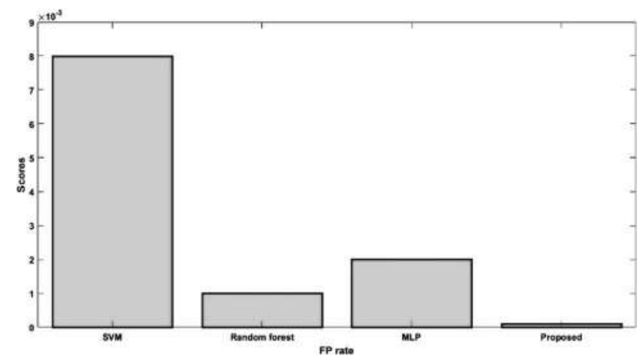

Fig. 19 False-positive rate analysis using Kaggle dataset

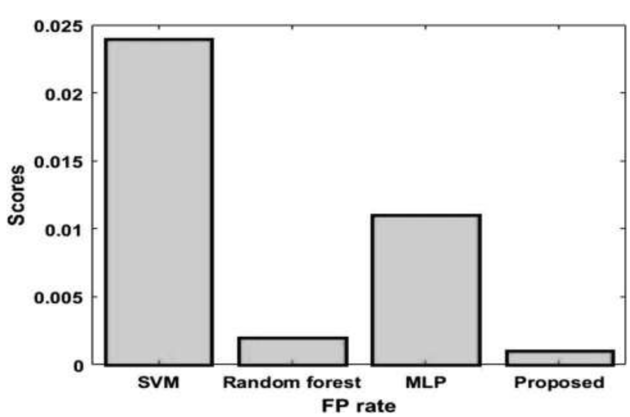

Fig. 18 False-positive rate analysis using MESSIDOR dataset

method into practice is to make the DR detection system less complex while consuming less time. Additionally, for precise DR prediction and stage categorization, the selected characteristics are loaded into the classifier known as the DMIC model. By using the benchmarking datasets such as DIARETDB1, MESSIDOR, IDRID, Kaggle, and EyePACS, the proposed Iter Net–based I^2WD-DMIC algorithm is validated and compared for performance assessment. The results show that, in comparison to existing machine learning models, the proposed DR detection model offers better results for all the datasets used in this study.

Author contribution Mr. Vinoth Rathinam: conceptualization, methodology, and writing—original draft preparation.

Mrs. Sasireka R: supervision.

Dr. K. Valarmathi: supervision.

Data availability Data sharing does not apply to this article as no new data has been created or analyzed in this study.

Declarations

Ethical approval and consent to participate This article does not contain any studies with human participants performed by any of the authors.

Consent for publication Not applicable.

Competing interests The authors declare no competing interests.

References

1. Özbay E. An active deep learning method for diabetic retinopathy detection in segmented fundus images using artificial bee colony algorithm. Artif Intell Rev. 2023;56(4):3291–318.
2. Wang X, Fang Y, Yang S, Zhu D, Wang M, Zhang J, Zhang J, Cheng J, Tong KY, Han X. CLC-Net: contextual and local collaborative network for lesion segmentation in diabetic retinopathy images. Neurocomputing. 2023;527:100–9.
3. Toğaçar M. Detection of retinopathy disease using morphological gradient and segmentation approaches in fundus images. Comput Methods Programs Biomed. 2022;214:106579.
4. Chen Y, Xu S, Long J, Xie Y. DR-Net: diabetic retinopathy detection with fusion multi-lesion segmentation and classification. Multimedia Tools App. 2023;82(17):26919–35.
5. Gargi M, Namburu A. An optimized intelligent boosting model for diabetic retinopathy segmentation severity analysis using fundus images. Eng Appl Sci Res. 2023;50(2):163–75.
6. Zhu W, Qiu P, Lepore N, Dumitrascu OM, Wang Y. Self-supervised equivariant regularization reconciles multiple-instance learning: joint referable diabetic retinopathy classification and lesion segmentation. In18th Int Symp Med Inf Process Anal. 2023;12567:100–7 (SPIE).
7. Solano A, Dietrich KN, Martínez-Sober M, Barranquero-Cardeñosa R, Vila-Tomás J, Hernández-Cámara P. Deep learning architectures for diagnosis of diabetic retinopathy. Appl Sci. 2023;13(7):4445.
8. Dayana AM, Emmanuel WS, Linda CH. Feature fusion and optimization integrated refined deep residual network for diabetic retinopathy severity classification using fundus image. Multimedia Syst. 2023;29(3):1629–50.
9. Vij R, Arora S. A systematic review on diabetic retinopathy detection using deep learning techniques. Arch Comput Methods Eng. 2023;30(3):2211–56.
10. Kaliaperumal K, Subramanian K, Thirunavukkarasu R, Varadharajan RK, Binsuwaidan R, Alabdallah NM, Alshammari N, Saeed M, Anbarasu K, Karunakaran R. Antibacterial wound dressing with hydrogel from chitosan and polyvinyl alcohol from the red cabbage extract loaded with silver nanoparticles. Green Process Synth. 2023;12(1):20230035.
11. Kaliaperumal K, Salendra L, Liu Y, Ju Z, Sahu SK, Elumalai S, Subramanian K, M. Alotaibi N, Alshammari N, Saeed M, Karunakaran R. Isolation of anticancer bioactive secondary metabolites from the sponge-derived endophytic fungi Penicillium sp. and in-silico computational docking approach. Front Microbiol. 2023;14:1216928.
12. Jena PK, Khuntia B, Palai C, Nayak M, Mishra TK, Mohanty SN. A novel approach for diabetic retinopathy screening using asymmetric deep learning features. Big Data Cogn Comput. 2023;7(1):25.
13. Shajin FH, Salini P, Rajesh P, Nagoji Rao VK. Efficient framework for brain tumour classification using hierarchical deep learning neural network classifier. Computer Methods Biomech Biomed Eng: Imag Vis. 2023;11(3):750–7.
14. Devi YA, Chari KM. Cascaded feature vector assisted blood vessel segmentation from retinal images. In: International Symposium on Intelligent Informatics 2022;241–254. Singapore: Springer Nature Singapore.
15. Errabih A, Benbah A, Nsiri B, Sadiq A, El Yousfi Alaoui MH, Oulad Haj Tham R, Benaji B. Diagnostic system and classification of diabetic retinopathy using convolutional neural network. In: Proceedings of Fourth International Conference on Communication, Computing and Electronics Systems: ICCCES 2022 2023;597–611. Singapore: Springer Nature Singapore.
16. Lee PK, Ra H, Baek J. Automated segmentation of ultra-widefield fluorescein angiography of diabetic retinopathy using deep learning. Br J Ophthalmol. 2023;107(12):1859–63.
17. Baskaran NK, Mahesh TR. Performance analysis of deep learning based segmentation of retinal lesions in fundus images. In2023 Second International Conference on Electronics and Renewable Systems (ICEARS) 2023;1306–1313. IEEE. https://doi.org/10.1109/ICEARS56392.2023.10085616.
18. Beevi SZ. Multi-Level severity classification for diabetic retinopathy based on hybrid optimization enabled deep learning. Biomed Signal Process Control. 2023;84:104736.
19. Jayachandran A, Kumar SR, Perumal TS. Multi-dimensional cascades neural network models for the segmentation of retinal vessels in colour fundus images. Multimedia Tools Appl. 2023;82(27):42927–43.
20. Kuna SL, Prasad AK, Bulla S. Meta heuristic fusion model for classification with modified U-Net-based segmentation. Int J Adv Comput Sci Appl. 2023;14(3). https://doi.org/10.14569/IJACSA.2023.0140388.
21. Liu R, Gao S, Zhang H, Wang S, Zhou L, Liu J. MTNet: A combined diagnosis algorithm of vessel segmentation and diabetic retinopathy for retinal images. PLoS ONE. 2022;17(11):e0278126.
22. Swetha D, Srilakshmi BL, Swami PS, Kumar KS, Priya MB. Review on blood vessel segmentation of retina from fundus images. In 2023 Second International Conference on Electronics and Renewable Systems (ICEARS). 2023;1472–1476. IEEE. https://doi.org/10.1109/ICEARS56392.2023.10085099.
23. Skouta A, Elmoufidi A, Jai-Andaloussi S, Ouchetto O. Hemorrhage semantic segmentation in fundus images for the diagnosis of diabetic retinopathy by using a convolutional neural network. J Big Data. 2022;9(1):78.
24. Shaukat N, Amin J, Sharif M, Azam F, Kadry S, Krishnamoorthy S. Three-dimensional semantic segmentation of diabetic retinopathy lesions and grading using transfer learning. J Personalized Med. 2022;12(9):1454.
25. Qummar S, Khan FG, Shah S, Khan A, Shamshirband S, Rehman ZU, Khan IA, Jadoon W. A deep learning ensemble approach for diabetic retinopathy detection. Ieee Access. 2019;7:150530–9.
26. Alyoubi WL, Shalash WM, Abulkhair MF. Diabetic retinopathy detection through deep learning techniques: a review. Inf Med Unlocked. 2020;20:100377.
27. Atwany MZ, Sahyoun AH, Yaqub M. Deep learning techniques for diabetic retinopathy classification: A survey. IEEE Access. 2022;10:28642–55.
28. Kandel I, Castelli M. Transfer learning with convolutional neural networks for diabetic retinopathy image classification. Rev Appl Sci. 2020;10(6):2021.
29. Kassani SH, Kassani PH, Khazaeinezhad R, Wesolowski MJ, Schneider KA, Deters R. Diabetic retinopathy classification using a modified Xception architecture. In2019 IEEE international symposium on signal processing and information technology (ISSPIT) 2019;1–6. IEEE. https://doi.org/10.1109/ISSPIT47144.2019.9001846.

30. Shanthi T, Sabeenian RS. Modified AlexNet architecture for classification of diabetic retinopathy images. Comput Electr Eng. 2019;76:56–64.
31. Huang S, Li J, Xiao Y, Shen N, Xu T. RTNet: relation transformer network for diabetic retinopathy multi-lesion segmentation. IEEE Trans Med Imaging. 2022;41(6):1596–607.
32. Sambyal N, Saini P, Syal R, Gupta V. Modified U-Net architecture for semantic segmentation of diabetic retinopathy images. Biocybernetics Biomed Eng. 2020;40(3):1094–109.
33. Hasan MK, Alam MA, Elahi MT, Roy S, Martí R. DRNet: Segmentation and localization of optic disc and Fovea from diabetic retinopathy image. Artif Intell Med. 2021;111:102001.
34. Kumar S, Adarsh A, Kumar B, Singh AK. An automated early diabetic retinopathy detection through improved blood vessel and optic disc segmentation. Opt Laser Technol. 2020;121:105815.
35. Xu Y, Zhou Z, Li X, Zhang N, Zhang M, Wei P. Ffu-net: feature fusion u-net for lesion segmentation of diabetic retinopathy. BioMed Res Int. 2021;2021. https://doi.org/10.1155/2021/6644071.
36. Saranya P, Prabakaran S, Kumar R, Das E. Blood vessel segmentation in retinal fundus images for proliferative diabetic retinopathy screening using deep learning. Vis Comput. 2022:1–6. https://doi.org/10.1007/s00371-021-02062-0.
37. Guo Y, Peng Y. CARNet: cascade attentive RefineNet for multi-lesion segmentation of diabetic retinopathy images. Complex Intell Sys. 2022;8(2):1681–701.
38. Sau PC, Bansal A. A novel diabetic retinopathy grading using modified deep neural network with segmentation of blood vessels and retinal abnormalities. Multimedia Tools Appl. 2022;81(27):39605–33.
39. Vinayaki VD, Kalaiselvi RJ. Multithreshold image segmentation technique using remora optimization algorithm for diabetic retinopathy detection from fundus images. Neural Process Lett. 2022;54(3):2363–84.
40. Yan H, Xie J, Zhu D, Jia L, Guo S. MSLF-Net: a multi-scale and multi-level feature fusion net for diabetic retinopathy segmentation. Diagnostics. 2022;12(12):2918.
41. Das S, Kharbanda K, Suchetha M, Raman R, Dhas E. Deep learning architecture based on segmented fundus image features for classification of diabetic retinopathy. Biomed Signal Process Control. 2021;68:102600.
42. Qiao L, Zhu Y, Zhou H. Diabetic retinopathy detection using prognosis of microaneurysm and early diagnosis system for non-proliferative diabetic retinopathy based on deep learning algorithms. IEEE Access. 2020;8:104292–302.
43. Gayathri S, Gopi VP, Palanisamy P. A lightweight CNN for diabetic retinopathy classification from fundus images. Biomed Signal Process Control. 2020;62:102115.